Received: 3 April 2019 | Revised: 26 December 2019 | Accepted: 13 January 2020
DOI: 10.1002/aoc.5554

FULL PAPER

Applied Organometallic Chemistry WILEY

Intercalation of copper salt to montmorillonite K-10 and its application as a reusable catalyst for Chan–Lam cross-coupling reaction

Manashi Sarmah[1] | **Anindita Dewan**[1] | **Purna K. Boruah**[2] | **Manash R. Das**[2] | **Utpal Bora**[1]

[1]Department of Chemical Sciences, Tezpur University, Tezpur, 784028, Assam, India

[2]Advanced Materials Group, Materials Sciences and Technology Division, CSIR-North East Institute of Science and Technology, Jorhat, 785006, Assam, India

Correspondence
Utpal Bora, Department of Chemical Sciences, Tezpur University, Tezpur 784028, Assam, India.
Email: utbora@yahoo.co.in; ubora@tezu.ernet.in

A simple and efficient catalytic system has been developed by adsorption of copper salt in the interlayers of montmorillonite K-10. The catalytic system impressively exercises the green chemistry perspective leading to effortless recovery and recyclability for the cross-coupling of arylboronic acids and N-nucleophiles. The effect of catalytic activity was studied for electronically diverse arylboronic acids and imidazoles relying on various optimizations under optimum thermal condition. The catalytic system was characterized and the morphology was determined.

KEYWORDS

arylboronic acid, copper sulfate, imidazole, montmorillonite

1 | INTRODUCTION

Transition metal-based catalysts serve as a valuable synthetic tool in the preparation of numerous industrially and medicinally important organic compounds.[1–3] The high cost of transition metals along with complex or difficult recovery on use as homogeneous catalysts has led to an interest in immobilizing transition metal catalyst onto supports. This heterogeneity can facilitate remarkable areas of opportunity in green chemistry, for example as robust support/stabilizer for synthesis, both the isolation and reusability of the catalyst providing environmentally suitable protocols. The stabilizer/support plays an important role in controlling the particle size, morphology, dispersion and activity of the catalyst.[4,5] As per global needs, industries demand the most practical, economically and environmentally viable manufacturing processes. In this respect, the application of natural and modified clays has emerged as novel supports for transition metal immobilization and are well documented in organic synthesis due to their versatile properties. Montmorillonite is the most important smectic (TOT or 2:1) structure which can form nanocomposites with various organic compounds. Along with both Brønsted and Lewis acid catalytic sites that allow alteration of the acidic nature of a material by a simple ion exchange method.[6] The applications of transition metals such as Ir, Ru, Fe and Au incorporated on nanoporous montmorillonite have been reported.[7–10] The incorporation of transition metals in solid supports has been intensively pursued for various organic transformations. Dutta and co-workers have reported the stabilization of Cu(0)-based nanoparticles into the nanopores of montmorillonite using acidic pretreatment followed by reduction with $NaBH_4$.[11] Previously we have reported the impregnation of Pd in montmorillonite pores and its catalytic potential was investigated in C–C cross-coupling reactions.[12,13] Similarly, in the work reported here, we studied the simple cation exchange properties of montmorillonite K-10 and subsequent adsorption of copper salt in the interlayer of its TOT smectic structure. We adopted a simple pretreatment of the clay which was subsequently interacted with $CuSO_4$ avoiding any vigorous or acid-treatment methodology.

https://doi.org/10.1002/aoc.5554
© 2020 John Wiley & Sons, Ltd.

Nitrogen-containing organic compounds such as N-aryl species are important intermediates of biologically active compounds with immense application in academia and industry, such as material sciences, agrochemicals, pharmaceuticals and synthetic chemistry.[14–19] Traditionally, various strategies have been adopted, and the most convenient and proven synthetic routes for installing N-aryl functionality are copper-catalyzed Ullman reaction[20] and palladium-promoted Buchwald–Hartwig amination.[21–25] Besides these, significant improvements for accessing these N-arylated derivatives have been made by Chan and co-workers and Collman and co-workers highlighting the wide applicability of copper source as catalyst.[26–29] Moreover, subsequent research efforts over the decades led to significant improvements in C–N coupling with various nucleophilic derivatives such as amides, oximes, sulfoximes and thiols co-catalyzed by additives such as TEMPO, molecular oxygen, pyridine-N-oxide, etc.[30–38] Considering the significance of N-aryl derivatives, we investigated the effect of copper sulfate-adsorbed montmorillonite in the C–N cross-coupling reactions of arylboronic acids and imidazoles. Moreover, the catalytic system was analyzed using inductively coupled plasma optical emission (ICP-OES), Fourier transform infrared (FT-IR) and solid-state UV spectroscopies, scanning electron microscopy (SEM), energy-dispersive X-ray (EDX) analysis, energy-dispersive spectroscopy (EDS) mapping and Brunauer–Emmett–Teller (BET) surface analysis. The cross-coupling products were isolated and characterized using FT-IR, ^{1}H NMR and ^{13}C NMR spectroscopies.

2 | EXPERIMENTAL

2.1 | General experimental procedure for preparation of copper catalyst

In a 100 ml round-bottom flask, 1 g of montmorillonite K-10 was mixed with 20 ml of tetrahydrofuran (THF). The mixture was then subjected to ultrasonication for 20 minutes and thereafter, THF was evaporated under reduced pressure. After complete evaporation of THF, 50 ml of methanol was added. The mixture was allowed to stir for 3 hours and then 0.05 g of $CuSO_4 \cdot 5H_2O$ was added to the solution. The resulting dispersion was then stirred under reflux conditions for 24 hours until the blue-colored solution became colorless. To ensure the maximum copper metal ion exchange, we additionally added 0.05 g of $CuSO_4 \cdot 5H_2O$ to the solution.[39] The solid obtained was washed with water and ethanol for several times and then centrifuged, after which the aqueous portion was subjected to ICP-OES analysis and the catalyst was dried under vacuum for 24 hours and stored at room temperature. The catalyst thus prepared was designated as Cu(II)@MMT.

2.2 | General procedure for N-arylation coupling reaction

To a 50 ml round-bottom flask, a mixture of imidazole (1 mmol), arylboronic acid (1.2 mmol), Cu(II)@MMT (20 wt%) and K_2CO_3 (1 mmol) in methanol (4 ml) was added and stirred at 60°C. The progress of the reaction was monitored via TLC. After completion, the reaction mixture was extracted with ethyl acetate (3 × 10 ml) and the combined organic layer was washed with brine (20 ml), dried over Na_2SO_4 and concentrated *in vacuo*. The residue was purified by column chromatography on silica gel (eluent: EtOAc–hexane, 1:1) to afford the corresponding N-arylated compound. The desired products were characterized by comparing ^{1}H NMR and ^{13}C NMR data with those of authentic samples (^{1}H and ^{13}C spectra are available in the supporting information).

2.3 | General procedure for recycling the catalytic system

The reusability of the catalytic system was investigated using imidazole (2 mmol) and phenylboronic acid (2.4 mmol) as coupling partners. After the first cycle, the reaction mixture was extracted with ethyl acetate followed by centrifugation. The clearly separated organic fraction was removed from the system and evaporated to afford the crude product. The remaining catalyst was washed with acetone and dried under vacuum and used for the next consecutive reaction cycle followed by addition of fresh reactants and solvent.

3 | RESULTS AND DISCUSSION

3.1 | Characterization of supported copper catalyst

ICP-OES analysis revealed that 5.9 wt% (0.0009 mol%) of copper sulfate was adsorbed in the interlayers of montmorillonite K-10 (0.1 g). Further, the structural/morphological features of Cu(II)@MMT were elucidated using SEM–EDX, powder X-ray diffraction (XRD), solid-state UV spectroscopy and BET surface analysis.

The FTIR spectrum of the parent montmorillonite (Figure 1a) shows an intense absorption band at *ca* 1044 cm^{-1} for Si—O stretching vibrations of a tetrahedral sheet. The bands at 797, 527 and 467 cm^{-1} were due to amorphous silica, Si—O—Al and Si—O—Si bending vibrations, respectively. And the absorption band at 3435 cm^{-1} is due to stretching vibrations of the OH groups. The FT-IR spectrum of the supported catalyst shows slight shift in absorption peak of the parent montmorillonite (Figure 1a).The absorption peak at 618.2 cm^{-1} is due to Cu—O vibration which is shifted from 616.8 cm^{-1} for

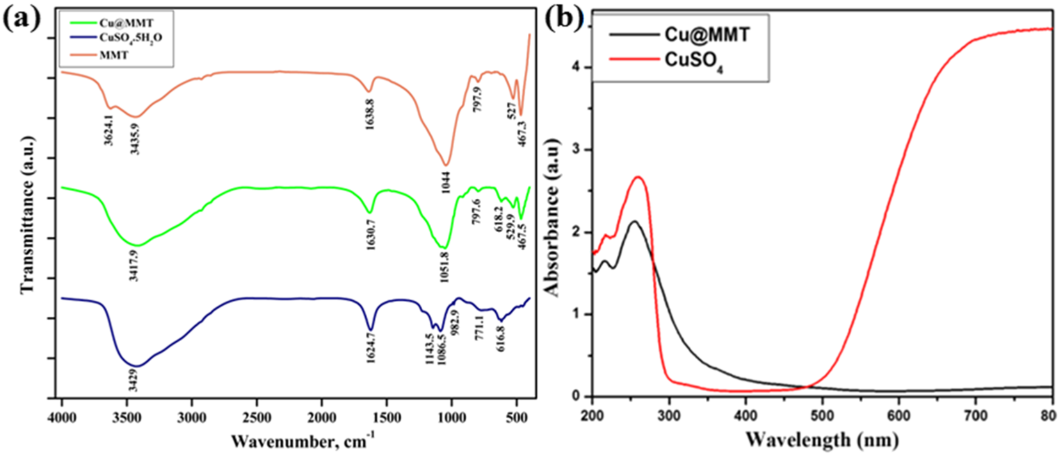

FIGURE 1 (a) FT-IR spectra of parent montmorillonite, Cu(II)@MMT and $CuSO_4{\cdot}5H_2O$. (b) UV–visible spectra of $CuSO_4$ and Cu(II)@MMT [Colour figure can be viewed at wileyonlinelibrary.com]

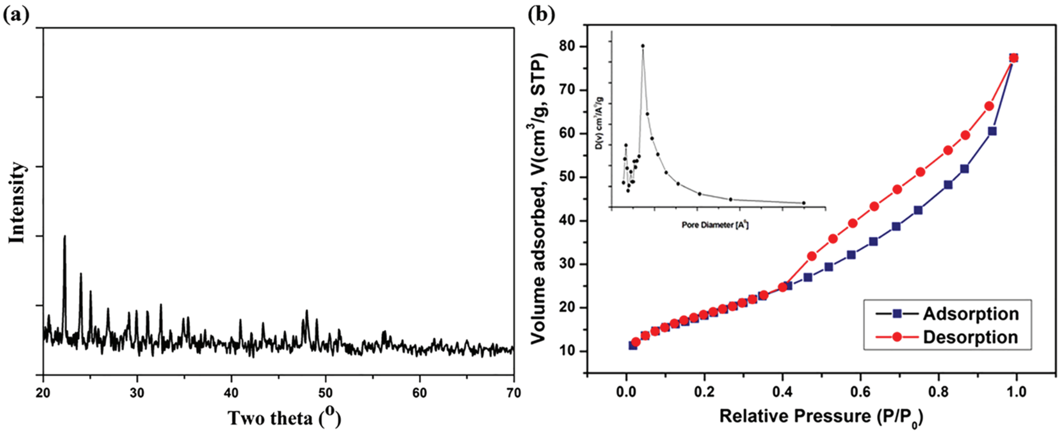

FIGURE 2 (a) Powder XRD pattern of Cu(II)@MMT. (b) Nitrogen adsorption–desorption isotherm and pore size distribution (inset) of Cu(II)@MMT [Colour figure can be viewed at wileyonlinelibrary.com]

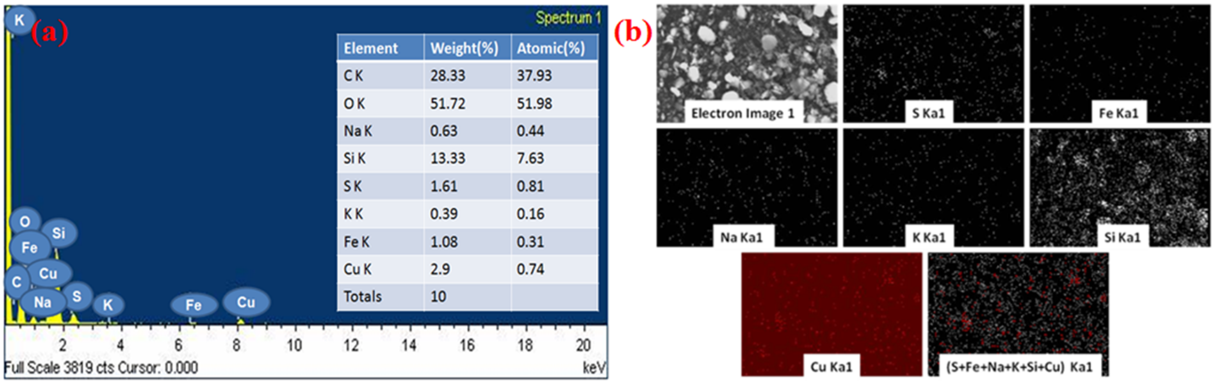

Element	Weight(%)	Atomic(%)
C K	28.33	37.93
O K	51.72	51.98
Na K	0.63	0.44
Si K	13.33	7.63
S K	1.61	0.81
K K	0.39	0.16
Fe K	1.08	0.31
Cu K	2.9	0.74
Totals	10	

FIGURE 3 (a) EDX analysis of Cu(II)@MMT. (b) SEM image and EDS mapping of Cu(II)@MMT [Colour figure can be viewed at wileyonlinelibrary.com]

$CuSO_4 \cdot 5H_2O$. The shifting of the band might possibly be due to the adsorption of $CuSO_4$ in the interlayers of montmorillonite.[12,40] Additionally, UV–visible absorption spectroscopy shows the difference in absorption shift of $CuSO_4$ and Cu(II)@MMT, thereby revealing the Cu—O interaction in the montmorillonite interlayer spacing (Figure 1b).[41]

The powder XRD pattern of the sample was recorded over a 2θ range of 10–70° (Figure 2a). The diffraction peaks resemble those of the crystal planes corresponding to $CuSO_4$ (JCPDS 802209). The pore characteristics and surface area of the prepared catalyst were examined using nitrogen adsorption and desorption analysis (BET). Prior to BET analysis the sample was degassed at 250°C for 3 hours. The corresponding adsorption–desorption isotherm and pore size distribution curve (inset) of the prepared catalyst are shown in Figure 2b. The pore size distribution curve was derived via the Barrett–Joyner–Halenda method. The isotherm belongs to type IV with an H3 hysteresis loop at P/P_0 of 0.4–0.99 which defines the mesoporosity of the material. The specific surface area of the catalyst was found to be 65.584 $m^2\ g^{-1}$, with an average pore diameter of 62.49 Å and pore volume of 0.102 $cm^3\ g^{-1}$, which is less than that of the parent montmorillonite K10 (surface area of 220–270 $m^2\ g^{-1}$), thereby indicating the adsorption of metal salt in the pores of montmorillonite.

EDX analysis of the catalyst shows the presence of Cu on the surface of modified montmorillonite along with the other elements of clay (Figure 3a). SEM study furnishes the surface topology and morphological evidence of the montmorillonite-embedded copper cations (Figure 3b). Furthermore, the precursor compound was assessed via EDS mapping which confirms the corresponding elemental distribution of the sample. The respective elemental mappings for (S + Fe + Na + K + Si + Cu) are presented in Figure 3b.

3.2 | Catalytic activity of Cu(II)@MMT in C–N cross-coupling reaction

The catalytic performance of Cu(II)@MMT was investigated for the coupling of imidazole (1 mmol) and arylboronic acid (1.2 mmol). Firstly, the activity of the

TABLE 1 Effect of Cu source and its amount on coupling reaction[a]

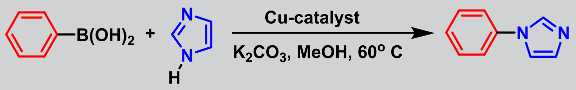

Entry	Copper source (mol%)	Time (h)	Yield (%)[b]
1	$CuSO_4 \cdot 5H_2O$ (5)	5	55
2	$CuSO_4 \cdot 5H_2O$ (10)	5	60
3	Cu $(NO_3)_2 \cdot 3H_2O$ (10)	5	60
4	Cu $(OAc)_2 \cdot H_2O$ (10)	5	65
5	$CuSO_4 \cdot 5H_2O$ (5) + MMT	4	69
6[d]	Cu(II)@MMT (20[c])	4	75
7	Cu(II)@MMT (20[c])	2	93
8	Cu(II)@MMT (5[c])	5	50
9	Cu(II)@MMT (15[c])	5	70
10	Cu(II)@MMT (25[c])	2	94

[a] Reaction conditions: imidazole (1 mmol), phenylboronic acid (1.2 mmol), K_2CO_3 (1 mmol), MeOH (4 ml), 60°C.

[b] Isolated yield.

[c] Weight percent of catalyst.

[d] 1 mmol of phenylboronic acid.

TABLE 2 Effect of various solvents and bases on C–N coupling reaction[a]

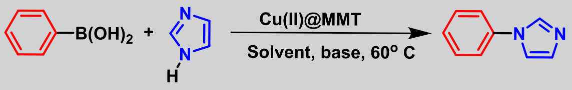

Entry	Solvent	Base	Time (h)	Yield (%)[b]
1	H_2O	K_2CO_3	4	71
2	MeOH	K_2CO_3	2	93
3	EtOH	K_2CO_3	3	87
4	EtOH–H_2O	K_2CO_3	4	75
5	MeOH–H_2O	K_2CO_3	4	80
6	i-PrOH	K_2CO_3	5	64
7	THF	K_2CO_3	6	<10
8	DMF	K_2CO_3	2	30
9	DMSO	K_2CO_3	2	30
10	MeOH	—	10	20
11	MeOH	NaOH	6	30
12	MeOH	Et_3N	6	35
13	MeOH	Cs_2CO_3	2	93
14[c]	MeOH	K_2CO_3	2	50
15[d]	MeOH	K_2CO_3	2	50

[a] Reaction conditions: imidazole (1 mmol), phenylboronic acid (1.2 mmol), base (1 mmol), solvent (4 ml), Cu(II)@MMT (20 wt%), 60°C.

[b] Isolated yield.

[c] 0.5 mmol of base.

[d] Room temperature.

TABLE 3 Coupling reaction of various arylboronic acids and imidazoles[a]

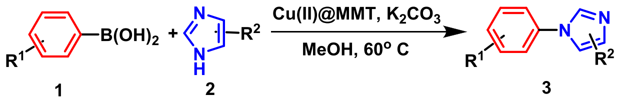

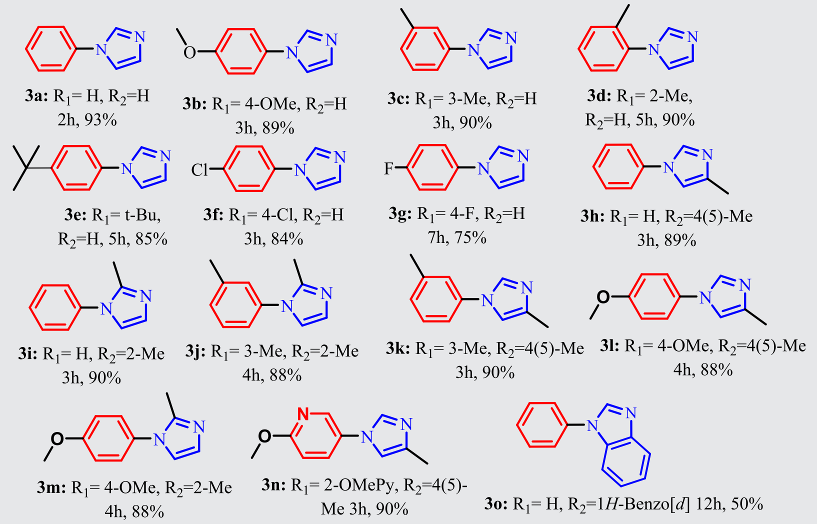

3a: R_1= H, R_2=H 2h, 93%

3b: R_1= 4-OMe, R_2=H 3h, 89%

3c: R_1= 3-Me, R_2=H 3h, 90%

3d: R_1= 2-Me, R_2=H, 5h, 90%

3e: R_1= t-Bu, R_2=H, 5h, 85%

3f: R_1= 4-Cl, R_2=H 3h, 84%

3g: R_1= 4-F, R_2=H 7h, 75%

3h: R_1= H, R_2=4(5)-Me 3h, 89%

3i: R_1= H, R_2=2-Me 3h, 90%

3j: R_1= 3-Me, R_2=2-Me 4h, 88%

3k: R_1= 3-Me, R_2=4(5)-Me 3h, 90%

3l: R_1= 4-OMe, R_2=4(5)-Me 4h, 88%

3m: R_1= 4-OMe, R_2=2-Me 4h, 88%

3n: R_1= 2-OMePy, R_2=4(5)-Me 3h, 90%

3o: R_1= H, R_2=1*H*-Benzo[*d*] 12h, 50%

[a] Reaction conditions: imidazole (1 mmol), phenylboronic acid (1.2 mmol), K_2CO_3 (1 mmol), MeOH (4 ml), Cu(II)@MMT (20 wt%), 60°C.

[b] Isolated yield.

catalyst was compared with that of homogeneous counterparts considering imidazole and phenylboronic acid as the model substrates; the results are presented in Table 1. We observed that the effectiveness of homogeneous copper salts towards the coupling reaction was significantly low (Table 1, entries 1–4). However, the reaction was slightly accelerated with the addition of montmorillonite with 5 mol% of $CuSO_4 \cdot 5H_2O$ (Table 1, entry 5). A considerable increase in reaction efficiency was observed using Cu(II)@MMT (Table 1, entries 6–10). On varying the amount of catalyst loading, appreciable alteration in reaction time and yield was noticed. Notably, there was excellent catalytic activity using 20 wt% of Cu(II)@MMT (Table 1, entry 7). On increasing the catalyst amount to 25 wt%, no significant difference in reaction yield was observed (Table 1, entry 10). Furthermore, varying the ratio of phenylboronic acid, we observed that the reaction performed efficiently with a 1:1.2 ratio of imidazole to arylboronic acid (Table 1, entries 6 and 7).

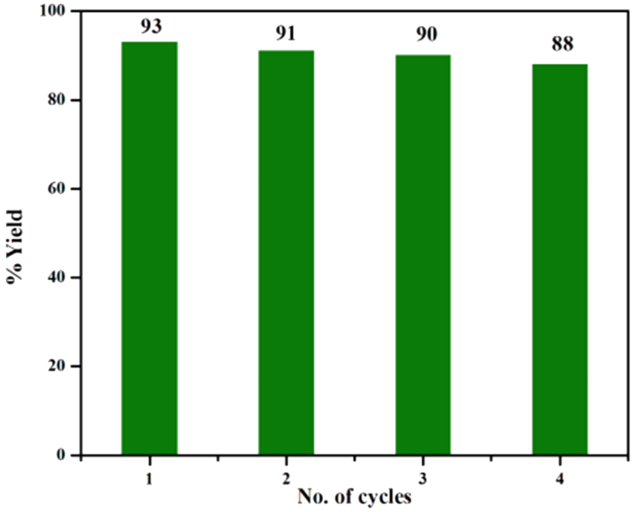

FIGURE 4 Reusability of the catalyst for coupling reaction [Colour figure can be viewed at wileyonlinelibrary.com]

It is well known that, in order to achieve the smooth progress of a reaction, solvent plays a key role. Various Chan–Lam reactions have been reported where methanol exhibits a superior activity over many organic solvents.[42–45] Based on these considerations, we next opted to study the effect of various solvents on the present catalytic system and the results are summarized in Table 2. On performing the reaction using 20 wt% Cu(II)@MMT in water, only 71% of the isolated product was obtained (Table 2, entry 1). On widening the solvent selection, we noticed that the reaction affords appreciable improvements in yield using organic and biphasic media (Table 2, entries 2–6). Excellent catalytic activity was achieved using methanol as sole medium (Table 2, entry 2). On the other hand, a markedly low yield of desired product was obtained in isopropyl alcohol (Table 2, entry 4). Reactivity of other protic and aprotic solvents was investigated but no appreciable result was obtained (Table 2, entries 7–9).

In addition to the above optimization, the role of base in the C–N coupling reaction is noteworthy. Base plays a significant role in the most crucial stage of the mechanism, the transmetalation stage, the transfer of the organoboron species to the metal cation. The reaction was performed in the absence of base but lower conversion to cross-coupling product was obtained (Table 2, entry 10). Thereafter, the reaction was screened using various bases. Among the bases examined, considerable low yield of cross-coupled product was obtained for NaOH and Et_3N (Table 2, entries 11 and 12). On the contrary, K_2CO_3 and Cs_2CO_3 provided excellent yield of N-arylated product (Table 2, entries 2 and 13). On lowering the amount of base and conducting the reaction at room temperature, a decrease in the product yield was obtained (Table 2, entries 14 and 15).

Next, the generality of this coupling of arylboronic acids with imidazoles was investigated using a variety of electronically diverse arylboronic acids and a wide range of imidazoles as substrates considering the optimized reaction conditions (Table 3). The catalytic system delivers excellent reactivity for both electron-withdrawing and electron-donating arylboronic acids (Table 3, 3**a**–3**o**). Imidazole with substituted group at varying positions reacts well (Table 3, 3**h**–3**n**). However benzimidazole directs the catalytic activity to considerably low conversion of isolated product along with longer reaction time (Table 3, 3**o**). From the aforementioned results, the catalytic system exhibits excellent performance for the N-arylation reaction.

3.3 | Recyclability of catalyst

On pursuing the principle of green chemistry, the major challenge of a catalytic system is its recyclability. So in an endeavor to expand the scope of this protocol, the reusability and efficiency of the catalytic system was investigated using imidazole and phenylboronic acid as coupling partners. Interestingly, the catalytic activity remains up to the fourth reuse which signifies the stability and efficient encapsulation of Cu(II) in montmorillonite interlayers (Figure 4). However, a decrease in reaction yield was observed in the fourth cycle which might due to loss of catalyst during recovery.

To confirm the heterogeneous nature of Cu(II)@MMT in the C–N cross-coupling reaction, we performed the hot filtration test considering the standard reaction conditions using imidazole and phenylboronic acid. The hot reaction mixture was filtered to remove the Cu(II)@MMT catalyst, the filtrate was allowed to further react and the progress of the reaction was monitored by TLC. Product formation was observed in the filtrate, which suggests a quasi-homogeneous process with a reversible dissolution–precipitation of Cu(II) species during the course of the reaction.[46,47]

To further confirm the structural stability and reusability of Cu(II)@MMT in the C–N coupling reaction, the recovered catalyst was characterized using powder XRD and field emission SEM. The powder XRD pattern of the sample was recorded over a 2θ range of 10–80° (Figure 5a). The diffraction peaks resemble those of the parent Cu(II)@MMT corresponding to crystal planes of $CuSO_4$. This was further confirmed using a morphological study: the SEM image of the reused catalyst in Figure 5b clearly shows the distribution of $CuSO_4$ crystals in the montmorillonite surface and interlayers. Additionally, EDX analysis confirms the presence of Cu in the catalyst after its reuse (Figure 5c).

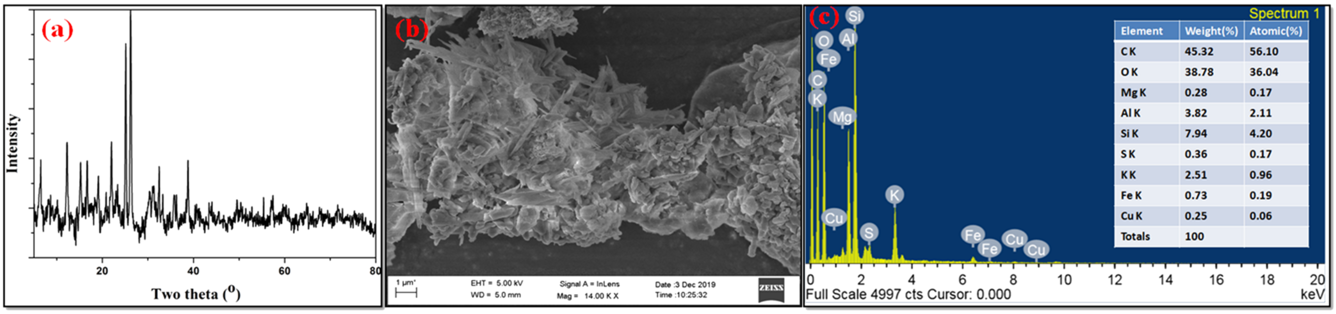

Element	Weight(%)	Atomic(%)
C K	45.32	56.10
O K	38.78	36.04
Mg K	0.28	0.17
Al K	3.82	2.11
Si K	7.94	4.20
S K	0.36	0.17
K K	2.51	0.96
Fe K	0.73	0.19
Cu K	0.25	0.06
Totals	100	

FIGURE 5 (a) Powder XRD pattern, (b) SEM image and (c) EDX analysis of recovered Cu(II)@MMT after the fourth cycle [Colour figure can be viewed at wileyonlinelibrary.com]

4 | CONCLUSIONS

Montmorillonite, which is an inexpensive and environmentally sustainable clay, proves to be an excellent host for the adsorption of copper sulfate. And this resourceful heterogeneousness actively surmounts the selective use of homogeneous catalysts. Moreover, the Cu(II)@MMT catalytic system shows excellent result with easy recovery and reuse. The system does not require environmentally unfavorable organic ligands, is less expensive and avoids protodeboronation of arylboronic acid. The robustness and simplicity of this heterogeneous catalyst makes it attractive for industrial application and also promising for researchers in the exploration of new synthetic strategies.

ACKNOWLEDGMENTS

The authors thank the Department of Science and Technology, New Delhi for providing financial support (no. EMR/2016/005944). M.S. thanks Tezpur University for providing an institutional fellowship and CSIR, New Delhi for financial assistance in the form of a CSIR-SRF fellowship. A.D. acknowledges DST, New Delhi for financial support. We are also grateful to Professor A. J. Thakur for fruitful discussions.

ORCID

Utpal Bora https://orcid.org/0000-0002-7403-0152

REFERENCES

[1] G. Jaouen, N. Metzler-Nolte, *Medicinal Organometallic Chemistry*, Vol. 32, Springer **2010**.

[2] P. A. Wender, F. C. Bi, G. G. Gamber, F. Gosselin, R. D. Hubbard, M. J. Scanio, R. Sun, T. J. Williams, L. Zhang, *Pure Appl. Chem.* **2002**, *74*, 25.

[3] A. D. Phillips, L. Gonsalvi, A. Romerosa, F. Vizza, M. Peruzzini, *Coord. Chem. Rev.* **2004**, *248*, 955.

[4] F. Schröder, D. Esken, M. Cokoja, M. W. Van Den Berg, O. I. Lebedev, G. Van Tendeloo, R. A. Fischer, *J. Am. Chem. Soc.* **2008**, *130*, 6119.

[5] S. F. Parker, H. C. Walker, S. K. Callear, E. Grünewald, T. Petzold, D. Wolf, P. W. Albers, *Chem. Sci.* **2019**, *10*, 480.

[6] N. Kaur, D. Kishore, *J. Chem. Pharm. Res.* **2012**, *4*, 991.

[7] P. Das, P. P. Sarmah, B. J. Borah, L. Saikia, D. K. Dutta, *New J. Chem.* **2016**, *40*, 2850.

[8] P. P. Sarmah, D. K. Dutta, *Green Chem.* **2012**, *14*, 1086.

[9] P. K. Saikia, P. P. Sarmah, B. J. Borah, L. Saikia, K. Saikia, D. K. Dutta, *Green Chem.* **2016**, *18*, 2843.

[10] B. J. Borah, S. J. Borah, K. Saikia, D. K. Dutta, *Catal. Sci. Technol.* **2014**, *4*, 4001.

[11] B. J. Borah, D. Dutta, P. P. Saikia, N. C. Barua, D. K. Dutta, *Green Chem.* **2011**, *13*, 3453.

[12] A. Gogoi, S. J. Chutia, P. K. Gogoi, U. Bora, *Appl. Organometal. Chem.* **2014**, *28*, 839.

[13] A. Mahanta, P. K. Raul, S. Saikia, U. Bora, A. J. Thakur, *Appl. Organometal. Chem.* **2018**, *32*, e4192.

[14] M. L. Quan, P. Y. S. Lam, Q. Han, D. J. P. Pinto, M. Y. He, R. Li, C. D. Ellis, C. G. Clark, C. A. Teleha, J. H. Sun, R. S. Alexander, S. Bai, J. M. Luettgen, R. M. Knabb, P. C. Wong, R. R. Wexler, *J. Med. Chem.* **2005**, *48*, 1729.

[15] S. Ueda, M. Su, S. L. Buchwald, *J. Am. Chem. Soc.* **2012**, *134*, 700.

[16] B. Narasimhan, D. Sharma, P. Kumar, *Med. Chem. Res.* **2011**, *20*, 1119.

[17] H. Niedermeyer, J. P. Hallett, I. J. Villar-Garcia, P. A. Hunt, T. Welton, *Chem. Soc. Rev.* **2012**, *41*, 7780.

[18] F. E. Hahn, M. C. Jahnke, *Angew. Chem. Int. Ed.* **2008**, *47*, 3122.

[19] L.-A. Schaper, S. J. Hock, W. A. Herrmann, F. E. Kuhn, *Angew. Chem. Int. Ed.* **2013**, *52*, 270.

[20] F. Ullmann, E. Illgen, *Ber. Dtsch. Chem. Ges.* **1914**, *47*, 380.

[21] B. P. Fors, N. R. Davis, S. L. Buchwald, *J. Am. Chem. Soc.* **2009**, *131*, 5766.

[22] J. F. Hartwig, *Synlett* **2006**, 1283.

[23] J. F. Hartwig, *Nature* **2008**, *455*, 314.

[24] J. F. Hartwig, *Acc. Chem. Res.* **2008**, *41*, 1534.

[25] P. Ruiz-Castillo, S. L. Buchwald, *Chem. Rev.* **2016**, *116*, 12564.

[26] D. M. T. Chan, K. L. Monaco, R.-P. Wang, M. P. Winters, *Tetrahedron Lett.* **1998**, *39*, 2933.

[27] P. Y. S. Lam, C. G. Clark, S. Saubernt, J. Adams, M. P. Winters, D. M. T. Chan, A. Combs, *Tetrahedron Lett.* **1998**, *39*, 2941.

[28] J. P. Collman, M. Zhong, *Org. Lett.* **2000**, *2*, 1233.

[29] J. P. Collman, M. Zhong, L. Zeng, S. Costanzo, *J. Org. Chem.* **2001**, *66*, 1528.

[30] S. A. Rossi, K. W. Shimkin, Q. Xu, L. M. Mori-Quiroz, D. A. Watson, *Org. Lett.* **2013**, *15*, 2314.

[31] S. Shi, R. Lalancette, R. Szostak, M. Szostak, *Org. Lett.* **2019**, *21*, 1253.

[32] M. Mondal, G. Sarmah, K. Gogoi, U. Bora, *Tetrahedron Lett.* **2012**, *53*, 6219.

[33] A. Hosseinian, L. Zare Fekri, A. Monfared, E. Vessally, M. Nikpassand, *J. Sulfur Chem.* **2018**, *39*, 674.

[34] W. Jiang, N. Li, L. Zhou, Q. Zeng, *ACS Catal.* **2018**, *8*, 9899.

[35] P. Y. S. Lam, G. Vincent, D. Bonne, C. G. Clark, *Tetrahedron Lett.* **2003**, *44*, 4927.

[36] T. D. Quach, R. A. Batey, *Org. Lett.* **2003**, *5*, 4397.

[37] X. Tang, W. Wu, W. Zeng, H. Jiang, *Acc. Chem. Res.* **2018**, *51*, 1092.

[38] K. Inamoto, K. Nozawa, J. Kadokawa, Y. Kondo, *Tetrahedron* **2012**, *68*, 7794.

[39] R. D. Aher, M. H. Gade, R. S. Reddy, A. Sudalai, *Indian J. Chem.* **2012**, *51A*, 1325.

[40] F. Gonella, F. Caccavale, L. D. Bogomolova, F. d'Acapito, A. Quaranta, *J. Appl. Phys.* **1998**, *83*, 1200.

[41] L. Cai, Y. Sun, W. Li, W. Zhang, X. Liu, D. Ding, N. Xu, *RSC Adv.* **2015**, *5*, 98136.

[42] J. B. Lan, L. Chen, X. Q. Yu, J. S. You, R. G. Xie, *Chem. Commun.* **2004**, *2*, 188.

[43] S. K. Das, P. Deka, M. Chetia, R. C. Deka, P. Bharali, U. Bora, *Catal. Lett.* **2018**, *148*, 547.

[44] M. L. Kantam, G. T. Venkanna, C. Sridhar, B. Sreedhar, B. M. Choudary, *J. Org. Chem.* **2006**, *71*, 9522.

[45] Z. H. Li, L. P. Xue, L. Wang, S. T. Zhang, B. T. Zhao, *Inorg. Chem. Commun.* **2013**, *27*, 119.
[46] T. Begum, M. Mondal, M. P. Borpuzari, R. Kar, P. K. Gogoi, U. Bora, *Eur. J. Org. Chem.* **2017**, 3244.
[47] M. Mondal, U. Bora, *Appl. Organometal. Chem.* **2014**, *28*, 354.

SUPPORTING INFORMATION

Additional supporting information may be found online in the Supporting Information section at the end of this article.

How to cite this article: Sarmah M, Dewan A, Boruah PK, Das MR, Bora U. Intercalation of copper salt to montmorillonite K-10 and its application as a reusable catalyst for Chan–Lam cross-coupling reaction. *Appl Organometal Chem*. 2020;e5554. https://doi.org/10.1002/aoc.5554